Supporting Information

Bioinspired Design of Strong, Tough and Thermally Stable Polymeric Materials *via* Nanoconfinement

Pingan Song,[*,†,‡] Jinfeng Dai,[†] Guorong Chen,[§] Youming Yu,[†] Zhengping Fang,[±] Weiwei Lei,[*,£] Shenyuan Fu,[†] Hao Wang[*,‡], and Zhi-Gang Chen[*,‡,∥]

[†]Department of Materials, Zhejiang A & F University, Hangzhou, 311300, China

[‡] Centre for Future Materials, University of Southern Queensland, Toowoomba, QLD 4350, Australia

[§] Research Centre of Nanoscience and Nanotechnology, Shanghai University, Shanghai, 200444, China

[±] Ningbo Institute of Technology, Zhejiang University, Ningbo, 315100, China

[£] Institute for Frontier Materials, Deakin University, Locked Bag 20000, Geelong, VIC 3220, Australia

[∥] Materials Engineering, the University of Queensland, Brisbane, QLD 4072, Australia

*Address correspondence to pingansong@gmail.com, weiwei.lei@deakin.edu.au, hao.wang@usq.edu.au, zhigang.chen@usq.edu.au.

Contents

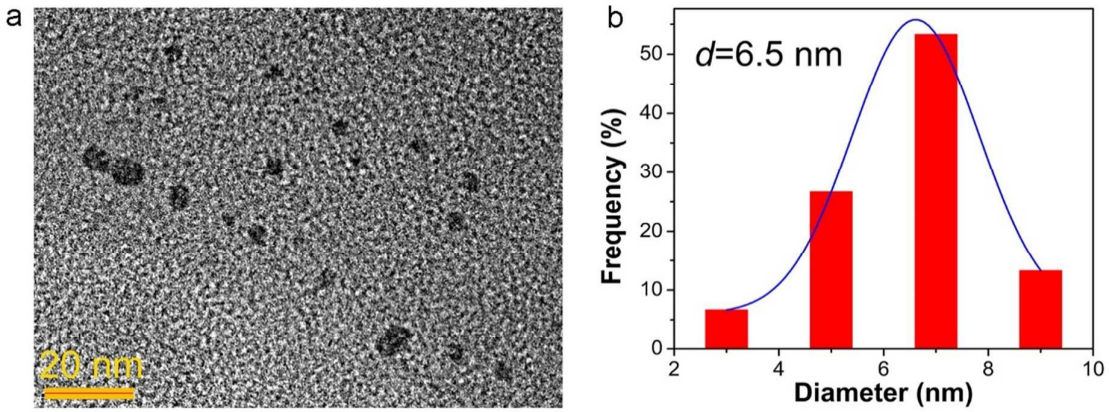

Figure S1. a) Typical transmission electronic microscopy image of as-prepared graphene oxide dots (GOD), demonstrating that the size of GOD is in the size range of 3-9 nm, with an average diameter of ~6.5 nm, and b) diameter distribution and pattern of as-prepared GOD, showing an average diameter of 6.5 nm, close to that of β-sheet of spider silk.

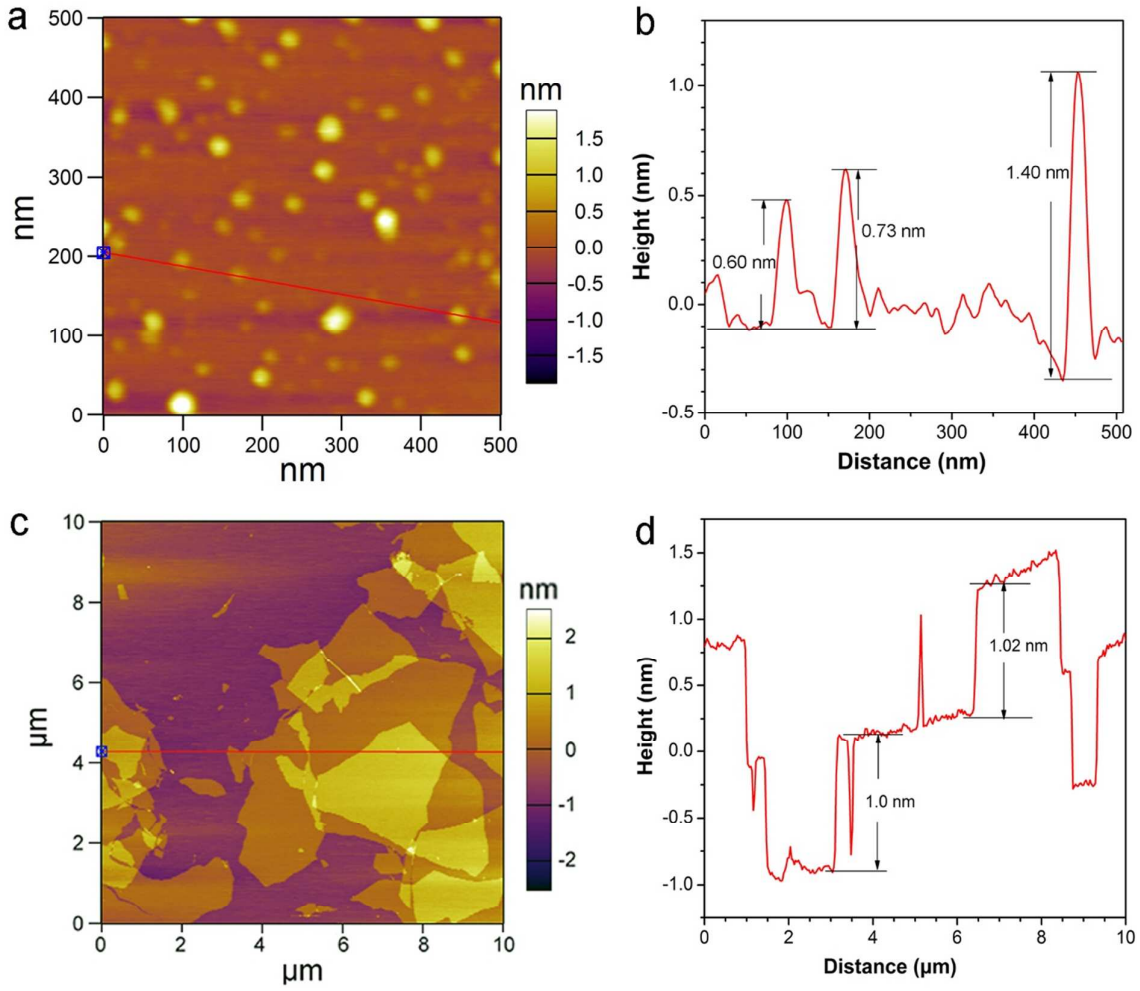

Figure S2. AFM image of as-prepared GOD and graphene oxides (GO), showing that GOD has a height of 0.60-0.73 nm indicating individual sheet whereas GO shows a typical thickness (height) of about 1.0 nm and a diameter range of 1-5 μm.

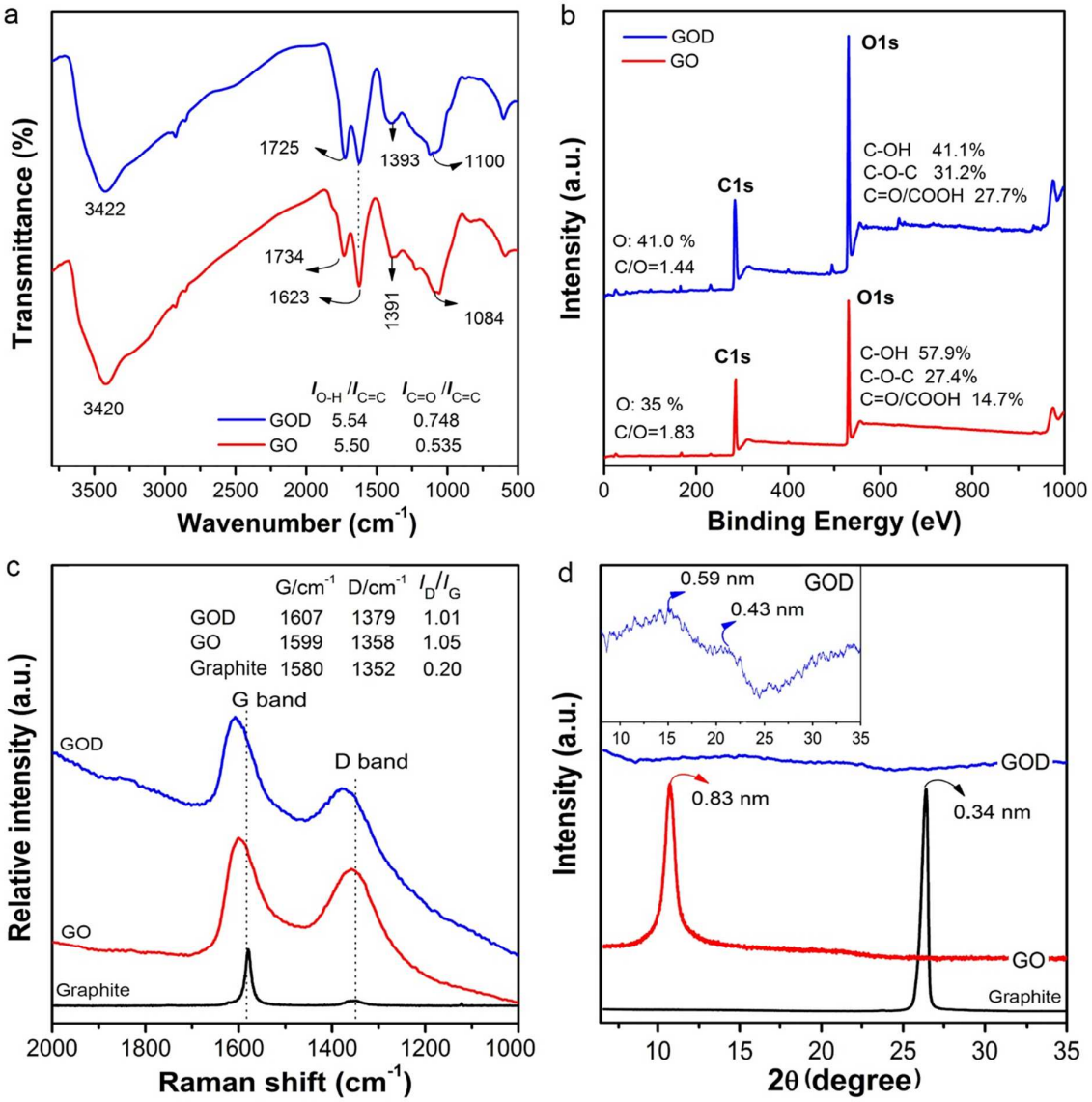

Figure S3. a) Infrared spectra (IR), b) X-ray photoelectron spectroscopy (XPS), c) raman spectra and d) X-ray diffraction (XRD) patterns of as-prepared GOD and GO, with the pristine graphite as comparison.

The IR and XPS measurements clearly indicate the presence of numerous different oxygen-containing groups with an oxygen content as high as 41.0 At.% in GOD (Figures S2a and S2b). The shift to high wavenumbers of both G band and D band further verifies the introduction of oxygen-containing groups in GOD after oxidation/cutting reactions (Figure S2c). Unlike the GO nanosheets, the interlayer space of GOD nearly cannot be determined by

the X-ray diffraction (XRD) because of its quantum size.

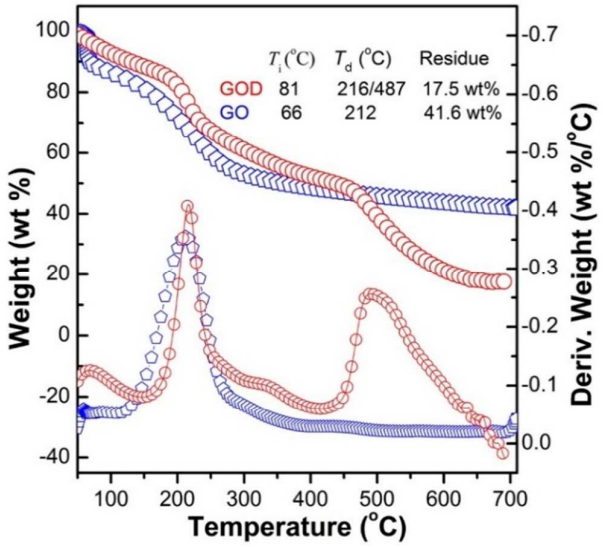

Figure S4. Thermogravimetric analysis (TGA) curves of as-prepared GOD and GO at a heating rate of 20 °C/min in nitrogen condition. T_i and T_d respectively represent the initial degradation temperature where 5 wt% weight loss takes place, and the maximum degradation temperature where the maximum weight loss occurs.

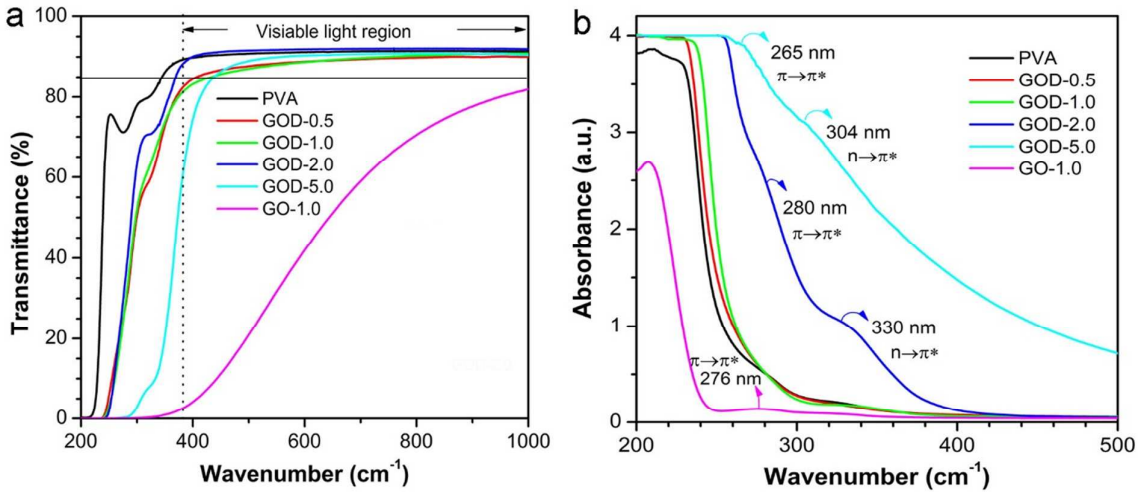

Figure S5. a) Typical UV-vis transmittance spectra and b) UV absorbance of PVA and its composite films based on GOD and GO with a film thickness of about 80 μm. All GOD composite films show higher transparency for GOD whereas the addition of GO reduces the transparency. GOD-2.0 and GOD-5.0 exhibit strong UV absorbance capability which is useful

for its outdoor application.

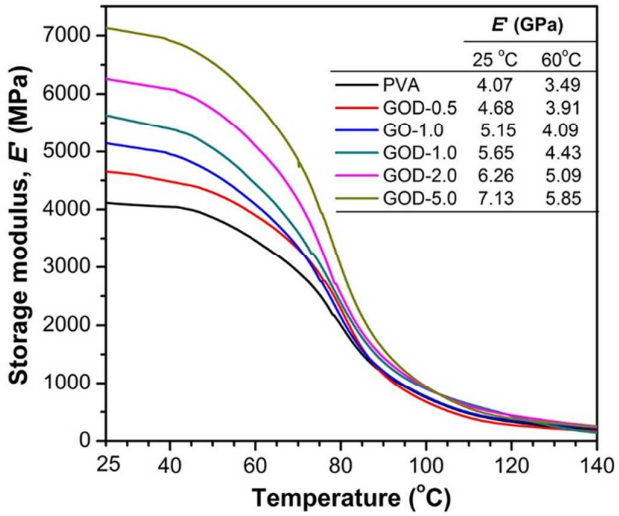

Figure S6. Temperature dependence of storage modulus (*E'*) of PVA and its composite films based on GOD and GO at a heating rate of 3°C/min, indicating that GOD can increase the storage modulus of PVA because of the nanoconfinement and hydrogen-bond crosslink effects. At the same loading level, GOD displays better reinforcing effects than GO in the entire testing temperature range.

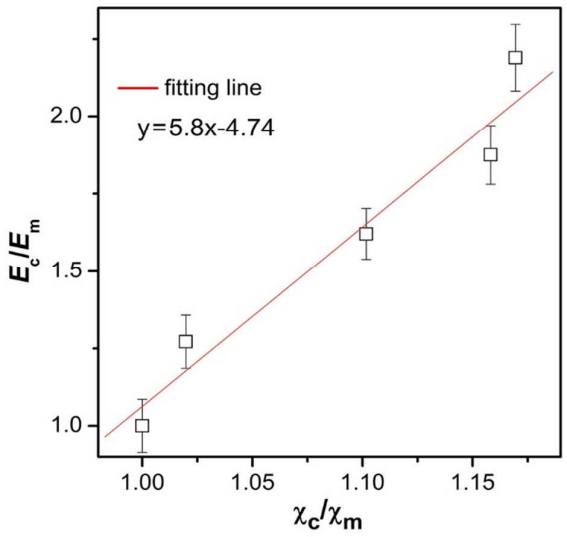

Figure S7. Relationships between relative *E* change (E_c/E_m) and relative degree change of

crystallinity (χ) (χ_c/χ_m), showing a good linear correlation.

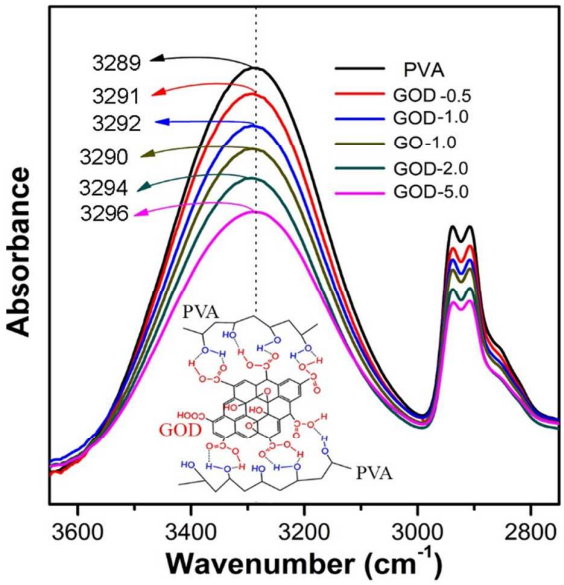

Figure S8. Stretching vibration of hydroxyl groups (O-H) of PVA and its composite films, showing strong intermolecular H-bond interactions between GOD and PVA, as evidenced by the blue shift of vibration peak of O-H groups.

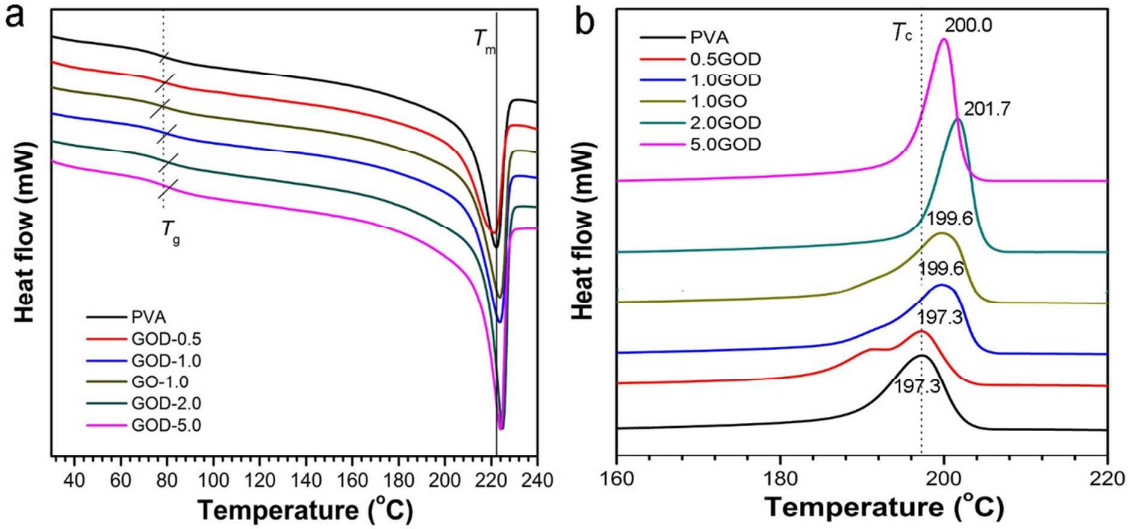

Figure S9. Differential scanning calorimetry (DSC) measurements of PVA and its composite films: a) heating cycle and b) cooling cycle at a heating/cooling rate of 10 °C/min, showing that the glass transition temperature (T_g) increases with increasing GOD content, whereas the crystallization temperature (T_c) also shifts to a higher temperature indicative of the promotion

effect of GOD and GO.

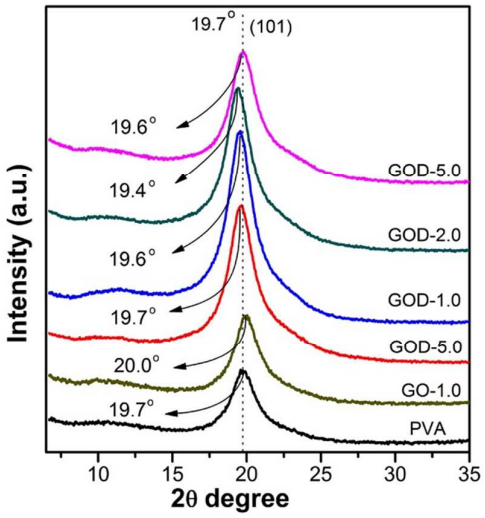

Figure S10. XRD diffraction patterns of PVA and its composite films based on GOD and GO, demonstrating that the presences of GOD and GO have no noticeable effect on the crystal form (101 crystal plane) of PVA.

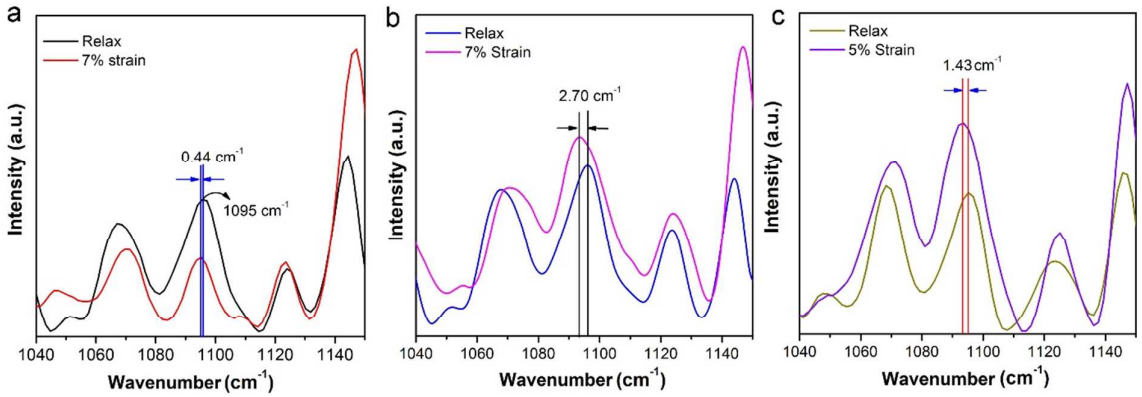

Figure S11. Raman spectra a) PVA, b) GOD-2.0, and c) GO-1.0, respectively showing a Raman shift of only 0.44 cm^{-1} for PVA, 2.7 cm^{-1} for GOD-2.0, and 1.43 cm^{-1} for GO-1.0. This is because the tensile stress leads to the deformation of C-O bonds in the PVA chains *via* H-bond interactions between PVA and GOD or GO.

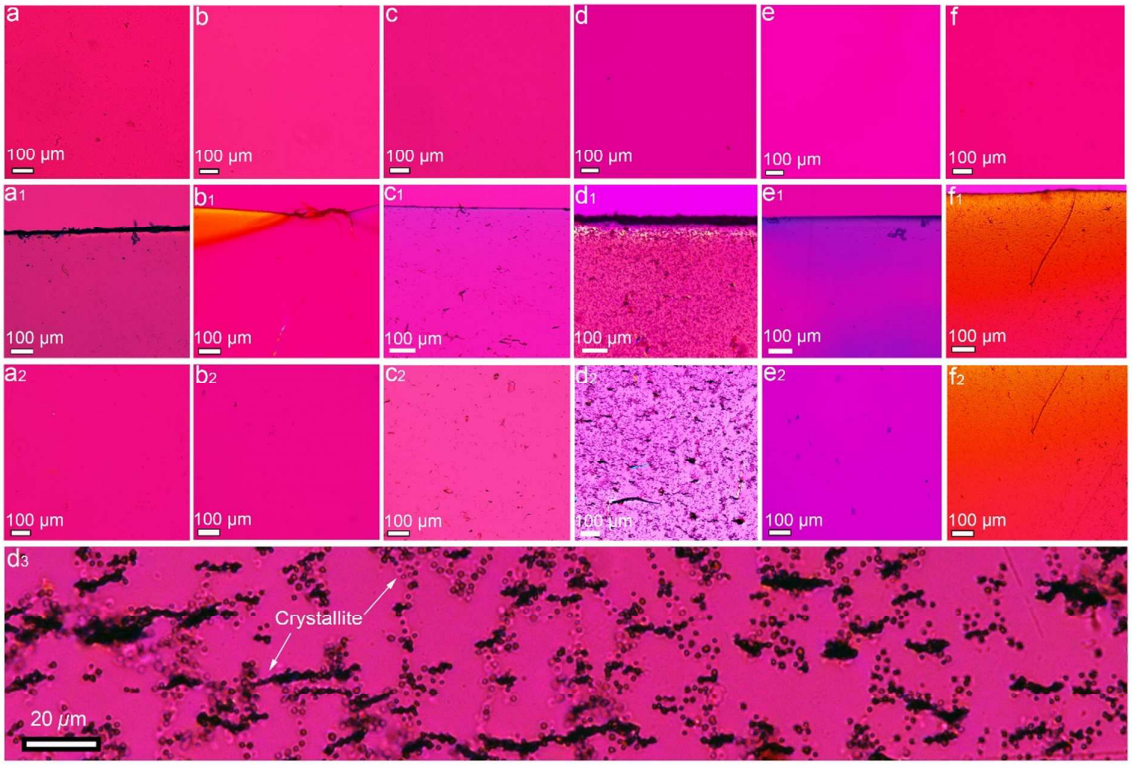

Figure S12. Polarized optical microscopy image of a, a_1, a_2) PVA, b, b_1, b_2) GOD-0.5, c, c_1, c_2) GOD-1.0, d, d_1-d_3) GOD-2.0, e, e_1, e_2) GOD-5.0, and f, f_1, f_2) GO-1.0. a-f) samples after tension, a_1-f_1) side surface the residual samples, a_2-f_2) side surface about 1 mm to the fracture section of samples after tensile failure, d_3 is the magnification (500×) part of d_2 (100×) of GOD-2.0, showing that GOD can act as a nucleating promoter to induce the crystallization of PVA during tensile process because of multiple H-bond interactions. The crystallites with an average size of around 1.0 μm formed during tension can also serve as physical giant cross-links, thus leading to increased mechanical strength and modulus.[S1]

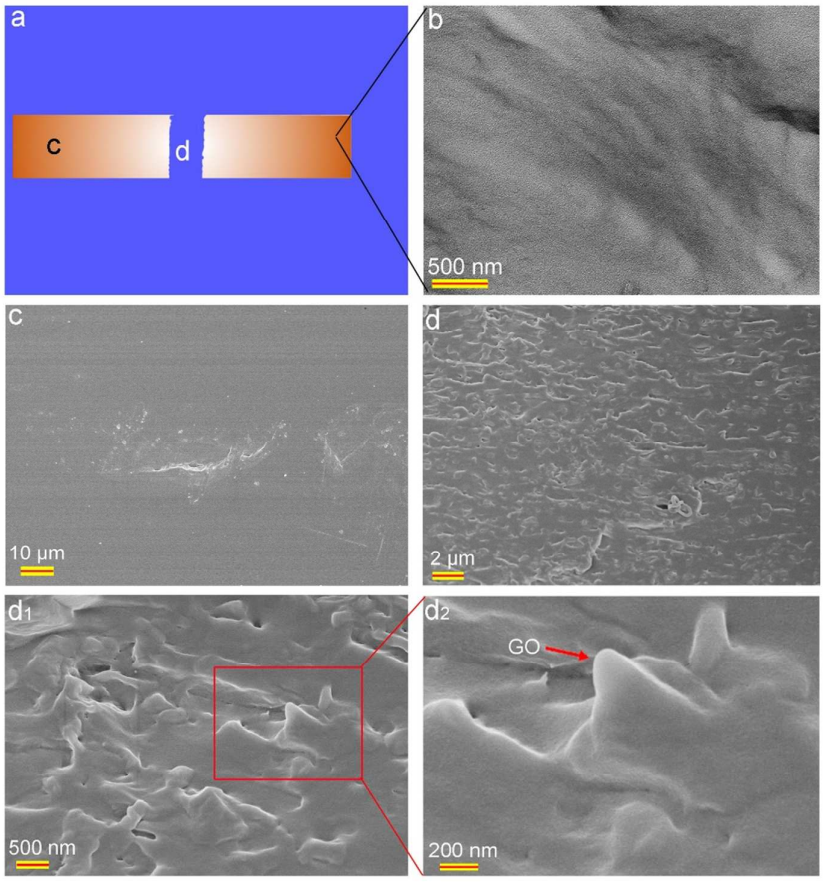

Figure S13. Typical transmission electron microscopy (TEM) and scanning electron microscopy (SEM) images of GO-1.0, a) the schematic representation of GO-1.0 film after tensile test, b) dispersion GO sheets within the PVA matrix, c) the surface of sample, and d, d_1, d_2) fracture morphology of the sample cross-section after tensile tests. The results show that the addition of GO makes PVA show a brittle fracture morphology despite homogeneous dispersion within the PVA matrix due to its large aspect ratio and weak interfaces with PVA.

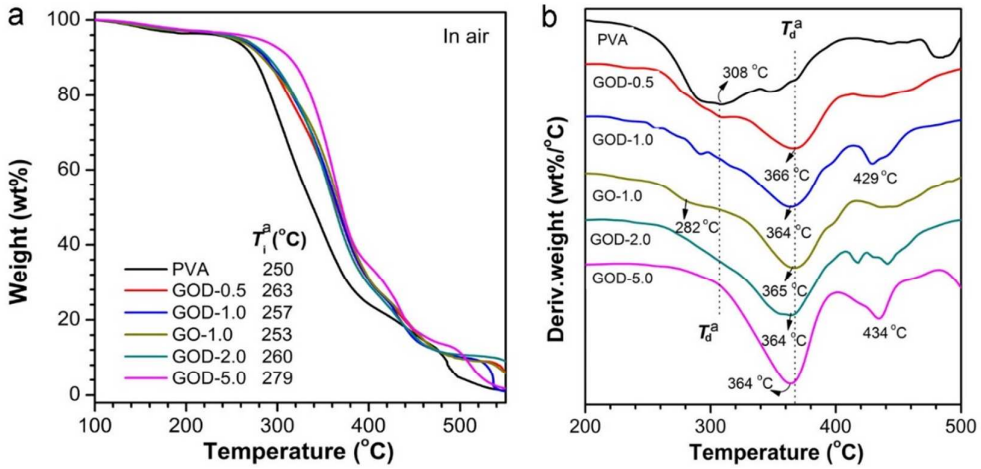

Figure S14. a) Typical thermogravimetric analysis (TGA) and b) derivative thermogravimetric weight loss (DTG) curves of the PVA matrix and its composite films filled with GOD and GO in air condition. T_i and T_d respectively represent the initial degradation temperature where 5 wt% weight loss takes place, and the maximum degradation temperature where the maximum weight loss occurs.

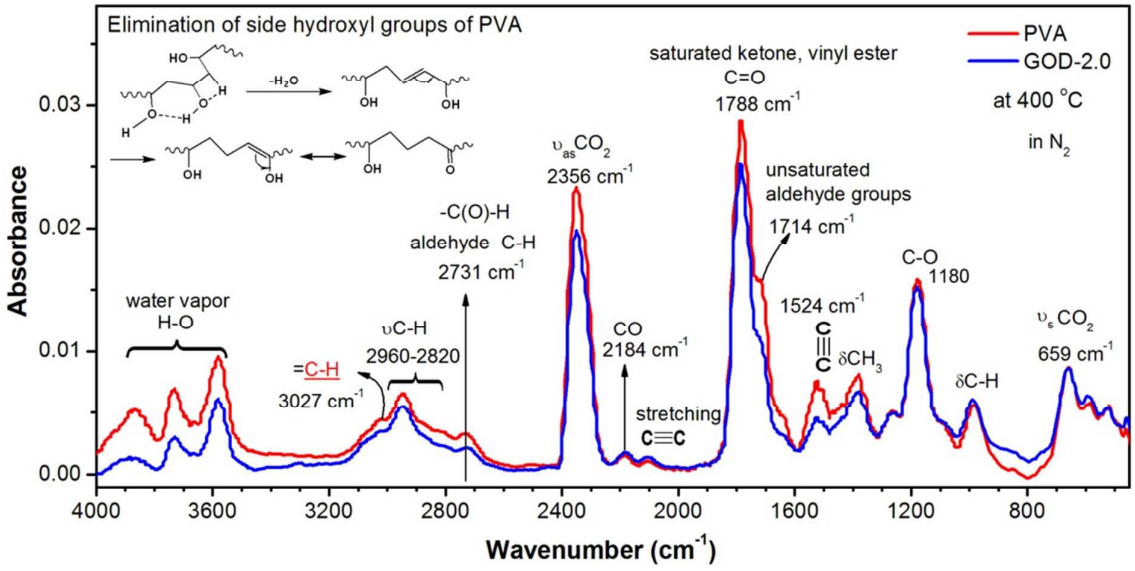

Figure S15. IR spectra of PVA and GOD-2.0 (the same mass) at 400 °C in N_2 atmosphere and the belongings of degradation products. GOD-2.0 clearly shows slower degradation and the evolution of fewer small degradation products during the heating process than the PVA matrix.

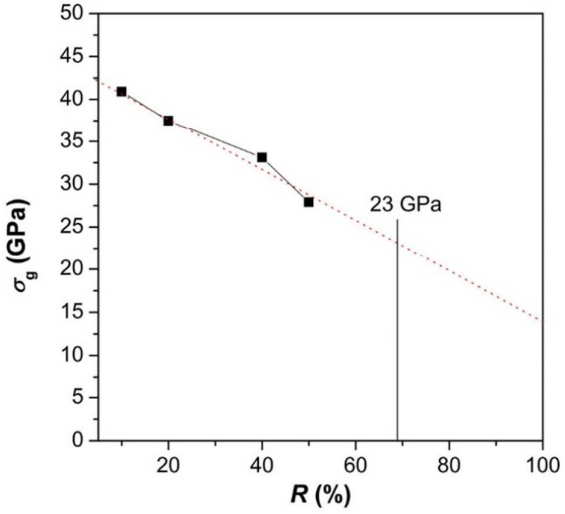

Figure S16. Theoretical prediction of tensile strength of as-prepared GOD, showing that as-prepared GOD with much higher oxygen content displays a tensile strength (σ_g) of around 23 GPa, much lower than the reported 130 GPa of graphene.[S2]

Table S1 Detailed thermal performances parameters obtained from DSC and TGA measurements.

Run	T_g [a] (°C)	T_g [b] (°C)	T_m [a] (°C)	ΔH_m [a] (J/g)	χ_c [a] (%)	T_i [c] (°C)	T_d [c] (°C)	E_a [d] (kJ/mol)
PVA	78.2	81.1	217	49.1	35.4	264	286	23.7
GOD-0.5	78.9	82.8	216	49.9	36.1	263	350	52.3
GOD-1.0	80.3	84.2	219	54.0	39.0	266	351	60.4
GO-1.0	75.2	80.0	219	53.8	38.9	261	277/356	48.1
GOD-2.0	80.8	87.3	220	56.7	41.0	272	355	80.0
GOD-5.0	81.5	88.4	219	57.3	41.4	290	357	114

[a] T_g, T_m, ΔH_m and χ refer to the glass transition temperature, melting point, and degree of crystallinity, repectively, obtained from DSC measurements. [b] T_g was obtained from DMA measurements. [c] T_i and T_d respectively represent the initial degradation temperature where 5 wt% weight loss takes place, and the maximum degradation temperature where the maximum weight loss occurs. [d] E_a represents the degradation activation energy of the sample at the T_d

temperature.

REFERENCES

(S1) Rault, J.; Marchal, J.; Judeinstein, P.; Albouy, P. A. Stress-Induced Crystallization and Reinforcement in Filled Natural Rubbers: ^{2}H NMR Study. *Macromolecules* **2006**, *39*, 8356-8368.

(S2) Liu, L. Z.; Zhang, J. F.; Zhao, J. J.; Liu, F. Mechanical Properties of Graphene Oxides. *Nanoscale* **2012**, 4, 5910-5916.